ELSEVIER

Biophysical Chemistry 124 (2006) 125–133

Biophysical Chemistry

http://www.elsevier.com/locate/biophyschem

Spectroscopic characterization of 2-amino-*N*-hexadecyl-benzamide (AHBA), a new fluorescence probe for membranes

Cássia Alessandra Marquezin [a], Izaura Yoshico Hirata [b], Luiz Juliano [b], Amando Siuiti Ito [a,*]

[a] *Departamento de Física e Matemática, Faculdade de Filosofia Ciências e Letras de Ribeirão Preto, Universidade de São Paulo, Av. Bandeirantes 3900 14040-901 Ribeirão Preto, SP, Brazil*

[b] *Departamento de Biofísica, Universidade Federal de São Paulo, Brazil*

Received 11 April 2006; received in revised form 9 June 2006; accepted 10 June 2006
Available online 14 June 2006

Abstract

We report the results of investigation on the spectroscopic properties of a new fluorescent lipophylic probe. The fluorophore *o*-aminobenzoic acid was covalently bound to the acyl chain hexadecylamine, producing the compound 2-amino-*N*-hexadecyl-benzamide. The behavior of the probe was dependent on the polarity of the medium: absorption and emission spectral position, quantum yield and lifetime decay indicate distinct behavior in water compared to ethanol and cyclohexane. The probe dissolves in the organic solvents, as indicated by the very low value of steady state fluorescence anisotropy and the short rotational correlation times obtained from fluorescence anisotropy decay measurements. On the other hand, the probe has low solubility in water, leading to the formation of aggregates in aqueous medium. The complex absorption spectrum in water was interpreted as originating from different forms of aggregation, as deduced from the wavelength dependence of anisotropy parameters. The probe interacts with surfactants in pre-micellar and micellar forms, as observed in experiments in the presence of sodium *n*-dodecylsulphate (SDS), *n*-cetyltrimethylammonium bromide (CTAB); 3-(dodecyl-dimethylammonium) propane-1-sulphonate (DPS) and 3-(hexadecyl-dimethylammonium) propane-1-sulphonate (HPS), and with vesicles of the phospholipid dimiristoyl-phosphatidylcholine (DMPC). The results demonstrate that AHBA is able to monitor properties like surface electric potential and phase transition of micelles and vesicles.

Keywords: Lipophilic fluorescent probe; Membranes; Fluorescent pH indicator; Electric surface potential; Vesicles phase transition

1. Introduction

An extrinsic probe with increased use in fluorescence studies of peptides is *ortho*-aminobenzoic acid (*o*-Abz). It has a structure comparable to those of natural amino acids and can be bound to the N^{α}-amino group of peptides without any significant change in its spectroscopic characteristics [1], usually maintaining high quantum yield, between 0.3 and 0.6 in water. Forming a pair with the acceptor molecule *N*-[2,4-dinitrophenyl]ethylenediamine (EDDnp), it is a convenient donor group in studies of internally quenched peptides which are substrates for proteases [2,3]. More recently, techniques based on Förster resonance energy transfer (FRET) were used to investigate conformational properties of fluorescent labeled bradykinin related peptides [4], heparin-binding peptides [5] and melanocyte stimulating hormone (MSH) peptides [6]. Donor–acceptor distance distributions were recovered from fluorescence decay profiles, which demonstrated the occurrence of conformational changes in the peptides in interaction with other compounds in the aqueous environment. Furthermore, it is important to note that, similar to many other fluorophores, *o*-Abz emission is dependent on the polarity of the medium and the probe was also used to monitor the interaction between bradykinin derived peptides and model membranes [7,8].

A considerable amount of fluorescent compounds have affinity to non-polar environment, or can be attached to fatty acids, phospholipids, steroids, and can probe the properties of different regions of model and biological membranes. In addition to the several probes of common use in membrane research, like lipophylic fluoresceins, lipophylic coumarins, diphenylhexatriene, laurdan, prodan, etc., many other compounds

* Corresponding author. Tel.: +55 16 602 3864; fax: +55 16 633 9949.
E-mail address: amandosi@ffclrp.usp.br (A.S. Ito).

0301-4622/$ - see front matter © 2006 Elsevier B.V. All rights reserved.
doi:10.1016/j.bpc.2006.06.002

have been recently reported as fluorescent probes for micelles and lipid bilayers. For example, an amino derivative of benzanthrone was investigated in its binding to liposomes and was proposed as a probe to study human peripheral blood mononuclear cells [9]. Absorption and emission properties of 2-hydroxy-substituted Nile Red (HONR) were examined in various solvents and micelles, showing differences in the binding site of the dye in cationic, anionic and nonionic micelles [10]. An aqueous soluble probe was synthesized which allowed the study of aggregation in micelles and polymeric micelles and the determination of critical micelle concentration (CMC) values at various surfactant compositions [11]. Also the new fluorescent probe 4-(2-pyren-1-yl-vinyl) pyridine responds to micelles and phospholipid vesicles of different surface charge, showing a large red-shift in the fluorescence emission when the surface charge of the organized media is anionic [12]. A methylamino derivative of pyrene incorporates in the micellar core and the emission is sensitive to the changes in surfactant concentration. Probe–surfactant interaction suggests the possible quantification of the chain length dependent premicellar aggregate formations [13].

Taking into account the spectroscopic properties of *o*-Abz, which made it a useful probe for peptides, we explored the possibility of its application as a fluorescent lipophilic probe. We synthesized the compound 2-amino-*N*-hexadecyl-benzamide (AHBA), where *o*-Abz is bound to long chain hexadecylamide, forming thus a fluorescent labeled alkyl chain (Scheme 1), which is intended to probe the surface region of membranes. The spectral properties of the newly synthesized compound were examined in different solvents: in buffer pH 7.4, representing the usual aqueous medium; in ethanol, a solvent less polar than water which present proton donor properties, a very important property to characterize specific interactions between solvent and probe; and also in cyclohexane, a non-protic solvent with very low polarity, representative of the interior of micelles and bilayers.

To characterize AHBA as a probe for membranes, we performed titration experiments with a series of surfactants which differ by the head group or by the acyl chain: Sodium *n*-dodecylsulphate (SDS), an anionic surfactant; the cationic *n*-cetyltrimethylammonium bromide (CTAB); 3-(dodecyl-dimethylammonium) propane-1-sulphonate (DPS), which has a zwitterionic head group and 3-(hexadecyl-dimethylammonium) propane-1-sulphonate (HPS), which has the same zwitterionic group bound to the long hexadecyl chain. To further assess the use of AHBA as a membrane probe we present also results of measurements in the presence of vesicles made of the phospholipid dimiristoyl-phosphatidylcholine (DMPC). The fluorescence parameters, both from steady state as time-resolved experiments, were employed to describe the interaction of the probe with micelles and vesicles, and to obtain information like surface potential and phase transition temperatures.

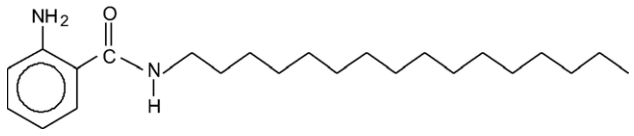

Scheme 1. Schematic representation of 2-amino-*N*-hexadecyl-benzamide (AHBA).

2. Materials and methods

Optical absorption measurements were performed using an Ultrospec 2100 (Amersham Pharmacia) UV/Visible spectrophotometer. For steady state fluorescence experiments we employed a SLM AMINCO 8100 spectrometer.

Time-resolved experiments were based on the time-correlated single photon counting method (TCSPC). The excitation source was a titanium-sapphire Spectra Physics laser, pumped by a Millenia X Spectra Physics laser. The pulses, at a repetition rate of 8000 kHz were tuned to give output from a third harmonic generator BBO crystal at 328 nm. They were directed to an Edinburgh F900 spectrometer and emitted photons were detected by a refrigerated Hamamatsu R3890U microchannel plate photomultiplier. Soleil-Babinet compensator in the excitation beam and a Glann-Thomson polarizer in the emission beam were used in anisotropy experiments. The FWHM of the instrument response function was typically 100 ps. Time resolution was 24 ps or 12 ps per channel in measurements of intensity decay or anisotropy decay, respectively. A software from Edinburgh Instruments was used to analyze the decay curves. The quality of fit was judged by statistical parameters like reduced χ^2 and by plot of residuals.

Organic solvents were from Merck, spectroscopic grade. Measurements in aqueous medium were performed in HEPES buffer 5 mM, pH 7.4 or phosphate buffer 5 mM, pH 7.4. Temperature was controlled using a Julabo refrigerating circulator. The surfactants SDS (sodium dodecyl sulfate), CTAB (hexadecyltrimethylammonium bromide), HPS (*N*-hexadecyl-*N*,*N*-dimethyl-3-ammonio-1-propanesulfonate) and DPS (*N*-dodecyl-*N*,*N*-dimethyl-3-ammonio-1-Propanesulfonate), were obtained from Sigma Chemical Co. (St. Louis, MO, USA). DMPC (1,2-dimyristoyl-*sn*-glycero-3-[phosphocholine]) was purchased from Avanti Polar Lipids (Birmingham, AL, USA).

2.1. Preparation of micelles and vesicles

Stock solutions of SDS, CTAB, HPS and DPS were prepared suspending the surfactant at the concentration of 0.5 M in Hepes buffer, 5 mM, pH 7.4. Small aliquots of the stock suspensions were added to the AHBA solutions to get the desired final surfactant/AHBA concentration ratio. Vesicles were obtained from the extrusion method [14]: a lipid film was formed from a chloroform solution of lipids, dried under a stream of N_2 and left under reduced pressure for a minimum of 2 h, to remove all traces of the organic solvent. Vesicles were prepared by the addition of the HEPES buffer to a concentration of lipid near 2 mM. The suspension was then extruded through polycarbonate membranes. The extrusion final step was made using 0.1 μm pore diameter polycarbonate membranes (from Millipore), resulting in large unilamellar vesicles (LUV).

3. AHBA synthesis

Abz-N ($C_{16}H_{34}$) was obtained by reaction of hexadecylamine with *N*-Boc-Abz-COOH using *O*-benzoil-1-yl-*N*,*N*,*N*′,*N*′-tetrametyluronium hexafluoroborate (TBTU) and hydroxibenzotriazol ($HOBt{\cdot}H_2O$), followed by treatment with TFA. The final deprotected compound was purified by semi-preparative HPLC using Econosil C-18 column (10 μM, 22.5 × 250 mn) and a two solvent system: (A) trifluoroacetic acid (TFA)/H_2O (1:1000) and (B) TFA/acetonitrile (ACN)/H_2O 1:900:100). The column was eluted at a flow rate of 5 mL/min with a 10 (or 30)–50 (or 60)% gradient of solvent B over 30 or 45 min. Analytical HPLC was performed using a binary HPLC system from Shimadzu with a SPD-10AV Shimadzu UV–VIS detector and a Shimadzu RF-535 fluorescence detector, coupled to an Ultrasphere C-18 column (5 μM, 4.6 × 150 mm) which was eluted with solvent system A1 (H_3PO_4/H_2O, 1:1000) and B1 (ACN/H_2O/H_3PO_4, 900:100:1) at a flow rate of 1.7 mL/min and a 10–80% gradient of B1 over 15 min. The HPLC column eluates were monitored by their absorbance at 220 nm and by fluorescence emission at 420 nm following excitation at 320 nm.

4. Results and discussion

4.1. Absorption and emission in solvents

Optical absorption and emission spectra in water, ethanol and cyclohexane are representative of electronic properties of AHBA in solvents with different polarity. Two absorption bands are discernible in the near UV absorption spectra of AHBA (Fig. 1), as usually observed in benzene derivatives [15]: one around 250 nm due to the $^1A \rightarrow L_a$ transition, and the other above 325 nm, originated from the $^1A \rightarrow L_b$ transition. In this work we pay attention to this last band related to the first excited state, which is involved with the fluorescence emission.

The results can be compared to those previously obtained for the free fluorophore and the *o*-Abz labeled peptides. It has been shown recently [16] that strong specific effects are present in the interaction of free *o*-Abz with proton donor solvents so that in water the absorption band occurs at 310 nm, strongly blue-shifted compared to absorption in cyclohexane, where the maximum is located at 338 nm. In *o*-Abz peptides the carbonyl of the fluorophore is covalently bound to the N^{α}-amino and the near UV band is positioned around 315 nm in water, with small shifts (2 nm) in organic solvents like ethanol and trifluoroethanol [4]. In the new probe AHBA, the same type of amide bond is present, however the presence of the long aliphatic chain prevents additional specific interaction with the solvent and absorption in non-polar solvent occurs at 327 nm (Table 1). On the other hand, the hydrophobic character of the aliphatic chain in AHBA causes very low solubility in water and the anomalous position (335 nm) of the UV absorption band in aqueous medium is attributed to the formation of aggregates. Contrary to expected from the general solvent effects, the value of Stokes shift in water is smaller than those in ethanol and cyclohexane. In this case, specific interactions between molecules in the aggregates originate the deviation from the linearity expected from the general solvent effects.

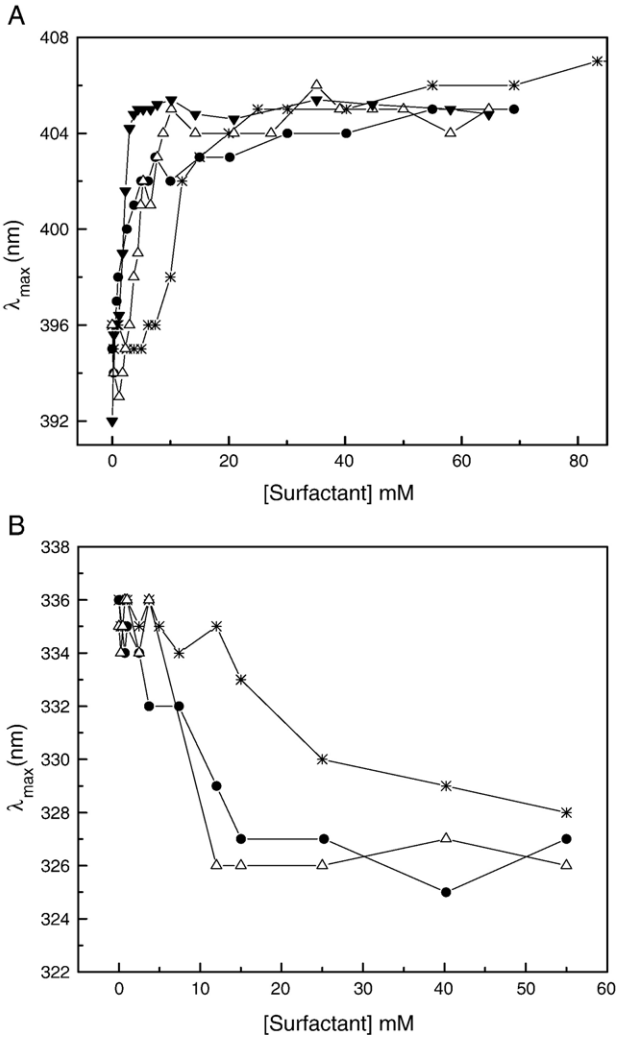

Fig. 1. Titration with surfactants SDS (∗), CTAB (●), DPS (△) and HPS (▼): changes in emission (A) and absorption (B) wavelengths. AHBA concentration: 10 μM.

Molar absorption coefficients are 2670 ± 72 cm^{-1} M^{-1} in water and 2960 ± 21 cm^{-1} M^{-1} in ethanol. The quantum yield (ϕ_f) of AHBA in aqueous solution and ethanol was calculated using the value 0.60 in ethanol as reference [17]. Values obtained were 0.38 and 0.78 in water and ethanol respectively. Energy homotransfer in the aggregates formed in water can contribute to decrease quantum yield of AHBA.

4.2. Titration with surfactants

In experiments of titration with SDS, CTAB, HPS and DPS, the absorption and emission spectra of AHBA gradually changed with the increase in surfactant concentration, so that the peak position moved to the values obtained for the probe in the organic solvents ethanol and cyclohexane (absorption in 326–328 nm and emission in 404–406 nm, Fig. 1). The results are indicative of the interaction of AHBA aggregates formed in water with the surfactant molecules, so that the probe assumes

Table 1
Position of $^1A \rightarrow L_b$ transition absorption band and of emission band in different solvents and values of Stokes shift

Compound	Solvent	λ_{absorb} (nm)	λ_{emiss} (nm)	$\Delta\nu$ ($\times 10^3$ cm^{-1})
o-Abz	Water	310	396	7.00
	Ethanol	335	407	5.28
	Cyclohexane	338	387	3.75
o-Abz-Pept.	Water/ethanol	314 to 316	415 to 418	7.71 to 7.37
AHBA	Water	335	395	4.53
	Ethanol	325	402	5.89
	Cyclohexane	327	402	5.70

monomer form and moves to regions of low polarity in the surfactant micelles. The spectral changes stabilize at concentrations above the surfactant CMC (0.01–0.06 mM for HPS, 1.0 mM for CTAB and 2.0–4.0 mM for DPS). And the titration plots show that the probe interacts with pre-micellar structures in the case of SDS, where the CMC is relatively high, around 7.0 mM.

Intensities are also sensitive to the changes in the environment around the probe. In the titrations the intensity rises continuously, even in surfactant concentration as low as 1.0 mM (Fig. 2). The interaction of AHBA with the pre-micellar forms of SDS, is observed as a small decrease in intensity before the increase which takes place above the CMC (7.0 mM).

Association constants were obtained from intensity titration curves, considering the interaction between probe and surfactant on a molecule-to-molecule basis. Then the association constant K_a comes from the equation

$$K_a = \frac{[\mathrm{AHBA} - S]}{[\mathrm{AHBA_f}][S_f]} \quad (1)$$

where $[\mathrm{AHBA} - S]$ and $[\mathrm{AHBA_f}]$ are the concentration of probe bound to surfactant and probe free, respectively, and $[S_f]$ is the concentration of free surfactant. The concentration of bound

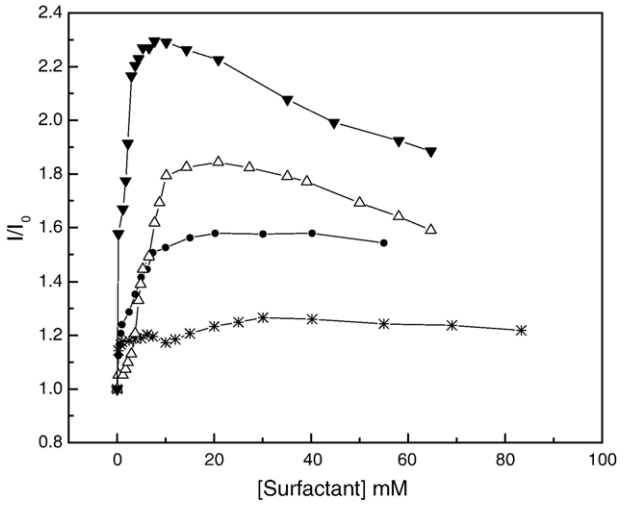

Fig. 2. Titration with surfactants SDS (∗), CTAB (●),and DPS (△): changes in intensity emission. AHBA concentration: 10 μM.

Table 2
Parameters obtained from the fit of titration curves to Eq. (2)

Surfactant	SDS	CTAB	HPS
K_a (mM)$^{-1}$	24.8±6.0	15.3±1.7	27.9±7.0
I_{max}	1.21±0.01	1.61±0.02	2.38±0.06

K_a is the association constants for the interaction of AHBA with surfactants.

probe was determined from the intensity of emission at different concentrations of surfactant. As the surfactants were always in excess compared to the probe, the concentration of free surfactant was approximated to the total concentration added in the titration experiments [7]. The association constant was then obtained from the equation which relates the intensity (I) to the total surfactant concentration [S]

$$\frac{I}{I_0} = 1 + \frac{K_a[S]}{1 + K_a[S]}\left(\frac{I_{max}}{I_0} - 1\right) \quad (2)$$

where I_0 is the fluorescence intensity in the absence of micelles and I_{max} is the maximum intensity corresponding to high surfactant concentration. The titration curves were fitted to this equation by non-linear square method, with K_a and I_{max} as adjustable parameters, and the results are shown in Table 2.

It was previously observed that the interaction of the free fluorophore *o*-Abz with micelles was dependent on the charge of the surfactant [18]. The interaction was strong with cationic CTAB micelles, weak with neutral *p-tert*-octylphenoxy-polyoxyethylene ether (TX100) and non-existent with SDS. As *o*-Abz was present in acidic form the results were interpreted in terms of electrostatic effects in the interaction. The importance of electrostatic effects was verified in studies of the interaction of SDS and *o*-Abz containing amino acids and peptides [7]: compounds with positive residues like Arg and Leu lead to association constants of 0.49 mM^{-1} and 0.44 mM^{-1} respectively. On the other hand, compounds with hydrophobic residues like Phe and Leu have slightly lower association constants, 0.24 mM^{-1} and 0.33 mM^{-1} respectively. As those residues are electrically neutral, the results show the importance of hydrophobic effects in the interaction.

The association constants obtained in this work for AHBA–surfactant interaction (Table 2) are considerably higher than reported previously for the free fluorophore and peptides labeled with *o*-Abz in interaction with SDS. As our titration experiments were performed at neutral pH, the probe is electrically neutral and hydrophobic effects should predominantly drive the interaction with surfactants. Despite of that, some minor effects are present, leading to smaller affinity of the probe for cationic CTAB, compared to anionic SDS or zwitterionic HPS.

4.3. Time-resolved fluorescence

Decay profiles were obtained at 400 nm with excitation at 328 nm. In ethanol the decay profile of AHBA is practically monoexponential (Fig. 3), dominated by a lifetime component of 6.71 ns with a small contribution from a 1.80 ns lifetime

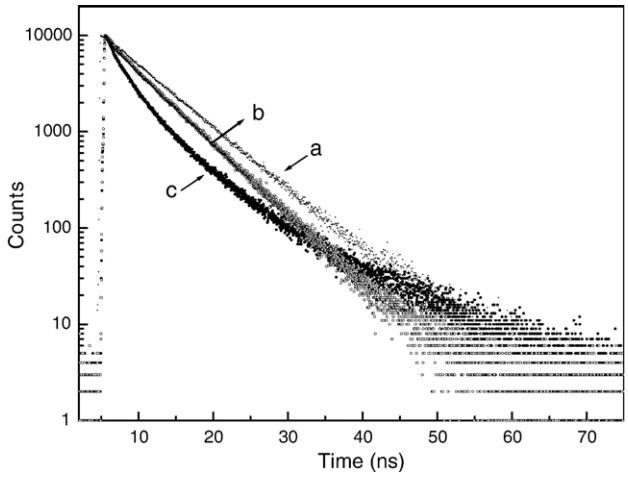

Fig. 3. Fluorescence intensity decay profiles of AHBA in ethanol (a), cyclohexane (b) and water (c). AHBA concentration 10 μM; excitation 328 nm and emission 400 nm.

component (Table 2). In cyclohexane the main component of 5.85 ns, showing a normalized pre-exponential factor of 0.77, was accompanied by minor contribution from a short lifetime of 0.90 ns. The decay of the probe in water is clearly more complex (Fig. 3) and could only be fitted to a three exponential curve with the most populated component (normalized pre-exponential factor of 0.52) having the intermediate lifetime value of 3.7 ns (Table 3).

The three lifetime components in water are related to complex aggregation of AHBA. Inside the aggregates formed in water, there must be an equilibrium between different isomeric forms of AHBA, with varied degrees of interaction between the amine, carbonyl and amide groups. That equilibrium can lead to more than one pathway for the deexcitation of the excited state, resulting in the heterogeneous fluorescence decay. Some heterogeneity in the decay is present also in cyclohexane, suggesting the occurrence of species where the fluorophore emission is quenched.

From the high quantum yield of AHBA in ethanol it could be expected a high value for its lifetime. However, the mean lifetime calculated as the intensity weighted average value ($\langle\tau\rangle = \sum_i \alpha_i\tau_i^2 / \sum_i \alpha_i\tau_i$, where α_i and τ_i are pre-exponential factor and lifetime of component i respectively), was only slightly above the values in water or cyclohexane. The values for the radiative lifetime calculated using the weighted average lifetime were then 8.6 and 13.8 ns in ethanol and water respectively. The numbers have the same order of magnitude as those for *o*-Abz in different solvents and for *o*-Abz peptides in water [1].

In the titration experiments we observed that the addition of surfactant did not affect greatly the values of the three lifetime components: the long (9.5–10.0 ns), the intermediate (3.0–4.0 ns) and the short (0.5–1.0) lifetimes are present in the deconvolution of the experimental decay (Table 3). However, the relative population of the lifetime components, expressed by the normalized pre-exponential factors, drastically changed in the presence of the micelles, and the contribution of the long lifetime becomes dominant (Table 3). As a result, the mean lifetime increases with the concentration of surfactant, as seen in Fig. 4. At high concentration of surfactant the percentile contribution of the short lifetime is lower than 2%. The contribution of the intermediate lifetime also decreases and the decay profiles are almost monoexponential.

Table 3
Parameters obtained from fitting of AHBA decay (10 μM) to multiexponential function in several conditions

	τ_1 (ns)	τ_2 (ns)	τ_3 (ns)	α_1	α_2	α_3	$\langle\tau\rangle$ (ns)
Ethanol	6.71	1.8	–	0.95	0.05	–	6.64
Cyclohexane	5.85	0.9	–	0.77	0.23	–	5.63
Water	10.0	3.7	1.3	0.10	0.52	0.38	5.25
SDS (30 mM)	9.42	3.1	0.32	0.70	0.08	0.22	9.01
CTAB (30 mM)	8.87	3.4	0.37	0.73	0.14	0.13	8.44
HPS (20 mM)	9.61	2.8	0.44	0.83	0.07	0.10	9.39
DMPC (0.5 mM)	9.41	4.3	1.3	0.40	0.39	0.21	7.52

Temperature: 25 °C. Errors: 0.06 for τ_1, 0.1 for τ_2 and 0.1 for τ_3, and 0.02 for α_i.

4.4. Fluorescence anisotropy

Steady state anisotropy measured at 26 °C was very low for the probes in cyclohexane (0.004±0.001) or ethanol (0.0060±0.0005), at probe concentrations up to 130 μM. In buffer solution, the anisotropy was considerably higher: even at low concentration (5 μM) the anisotropy was already 0.060, increasing to values around 0.100 at probe concentration above 80 μM, evidencing the occurrence of aggregates in water.

Anisotropy decay of the probe was strongly dependent on the solvent. Sub-nanosecond decay was observed in the experiments in ethanol (0.22 ns) indicating that the probe was dissolved and freely rotating as monomer. Short rotational correlation time (0.135 ns) from the probe in monomeric form dominates the anisotropy decay in cyclohexane, with minor contribution of a rotational correlation time of 4.64 ns which may come from oligomeric species formed in the low polarity solvent possibly stabilized by interactions between the head

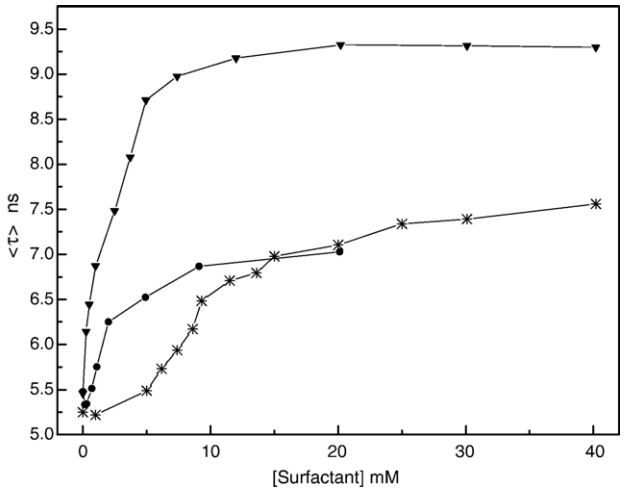

Fig. 4. Titration with surfactants SDS (∗), CTAB (●) and HPS (▼): changes in average weighted lifetimes. AHBA concentration: 10 μM.

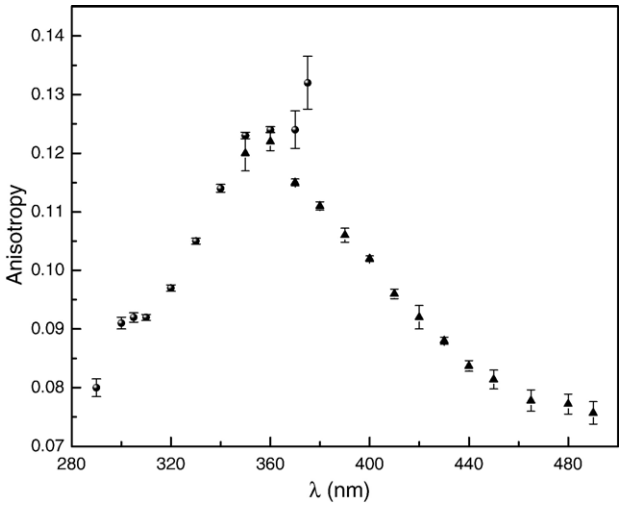

Fig. 5. Dependence of steady state anisotropy on excitation (emission at 400 nm) and emission (excitation at 328 nm) wavelength in buffer, pH 7.4, temperature 25 °C, AHBA concentration 140 μM.

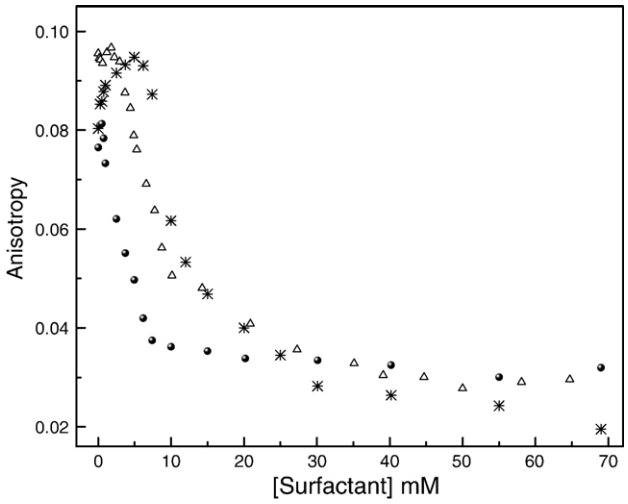

Fig. 6. Steady state anisotropy dependence with addition of surfactants SDS (∗), CTAB (●) and DPS (△). AHBA concentration 10 μM; excitation 328 nm and emission 400 nm.

groups of neighboring AHBA molecules. In water the anisotropy decay was fitted to a long rotational correlation time of 7.15 ns, reflecting the rotational diffusion, as a whole, of the aggregates formed in aqueous medium.

The steady state anisotropy in aqueous medium was observed to be dependent on the excitation wavelength: the absorption in the blue side of the band is related to anisotropies around 0.06 while excitation in the red side of the band results in higher values of anisotropy, around 0.10 (Fig. 5). This observation can be correlated to the broad absorption band of AHBA in water, anomalously red shifted compared to monomer absorption in polar solvents: within the aggregates there are several possibilities for the internal arrangement of the aromatic ring of the probe, leading to different interactions between the fluorophores, so that the complex absorption band should be the result of the superposition from different types of aggregates. The anisotropy dependence with the excitation wavelength reflects the contribution of species in the aggregates with different mobility or subjected to different internal depolarization processes.

The anisotropy of the AHBA aggregates is also dependent on the emission wavelength (Fig. 5). The same electronic state seems to be involved with the red side of the absorption band and the shorter wavelengths of the emission band. Correspondingly, excitation at shorter wavelength would be associated to the emission at longer wavelengths. No dependence with excitation or emission wavelength was observed in the probe in ethanol or cyclohexane, where the probe is predominantly present as monomer.

Addition of surfactants leads to an initial rise in anisotropy, followed by a continuous decrease towards values around 0.02–0.03 (Fig. 6). The initial increase reflects the progressive transformation of the AHBA aggregates, formed in aqueous medium, to complexes formed with surfactant pre-micellar structures, similar to the observed in the titrations examined by peak position, fluorescence intensity and lifetime ((Figs. 1, 2 and 4)). After concentrations above the CMC (1 mM for CTAB, 2–4 mM for DPS, 8 mM for SDS), the probe incorporates into the micelles and the anisotropy decreases to values dependent on the surfactant molecule. Higher final anisotropy was obtained for CTAB whose aggregation number (170) is larger than for DPS (55) and SDS (62).

Time-resolved anisotropy experiments were performed in the presence of SDS and CTAB. In the absence of surfactant the anisotropy decay was fitted to a monoexponential curve and the rotational correlation time was around 7 ns as obtained for the probe aggregates in water. After addition of surfactants, the experimental curves were fitted to a two component decay: a long correlation time, Φ_{long}, initially raised to 15 ns, due to the interaction with pre-micellar structures, and, above CMC, converged to 7.0 ns in CTAB and 5.5 ns in SDS (Fig. 7a), values which should be representative of the tumbling of the micelles; it also appeared a short component, Φ_{short} in Fig. 7b, which goes to 0.7 ns in CTAB and 0.4 in SDS at high

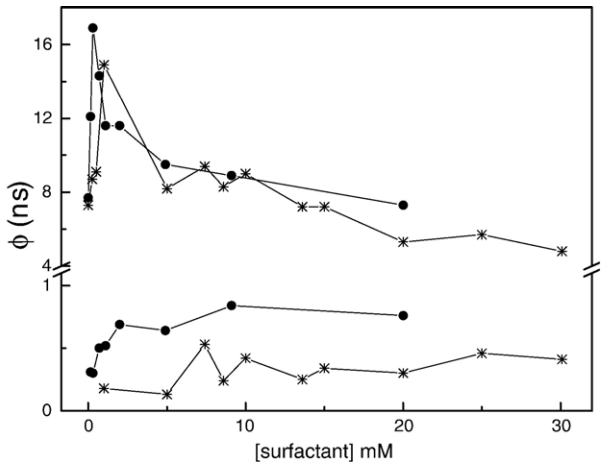

Fig. 7. Rotational correlation time dependence with addition of surfactants SDS (∗) and CTAB (●). AHBA concentration 10 μM; excitation 328 nm and emission 400 nm.

surfactant concentration, which are related to rotational diffusion of the probe in the micelles.

4.5. Interaction with DMPC vesicles: monitoring phase transition

Probe (10 μM) was added to DMPC vesicles (0.5 mM in phosphate buffer) prepared by extrusion method. Similar to the observed for the probe in the presence of surfactant micelles, the emission spectrum presented a peak at 404 nm. Time-resolved fluorescence intensity profiles were best fitted to three exponential decay curves and lifetimes decreased slightly with increase in temperature in the interval from 15 to 31 °C. The long lifetime ranged from 10.0 to 9.1 ns, the intermediate from 5.1 to 4.3 ns and the short from 1.7 to 1.3 ns (see Table 2 for values at 25 °C). The pre-exponential factors remained practically unchanged and calculated values of average intensity weighted lifetime suggests that the parameter is able to describe the fact that the above temperature interval spans the transition between the liquid crystal to the gel phase of the bilayer (Fig. 8).

Steady state anisotropy of AHBA in DMPC vesicles is relatively high (0.160) at low temperature (15 °C) and decreased to 0.060 at temperatures above 30 °C. The plot of anisotropy versus temperature (Fig. 9A) allows the discrimination of the transition from the liquid crystal phase to the gel phase of DMPC bilayer, and the determination of the phase transition temperature. The result, 22 °C is in good agreement with values reported in the literature [19].

Time-resolved anisotropy decay data were adjusted to bi-exponential curves. The long rotational correlation time, related to the rotation of the whole probe, was quite high at 15 °C (circa 12.0 ns) and diminished to circa 4.5 ns above 30 °C. The plot of the long correlation time versus temperature (Fig. 9B) also reflected the phase transition of the bilayer near to 22 °C. The short correlation time varied between 0.10 and 0.30 ns and was related to the movement of the fluorescent aromatic ring. We did not observe a definite trend with the variation of temperature, due to the relatively large errors associated to those times.

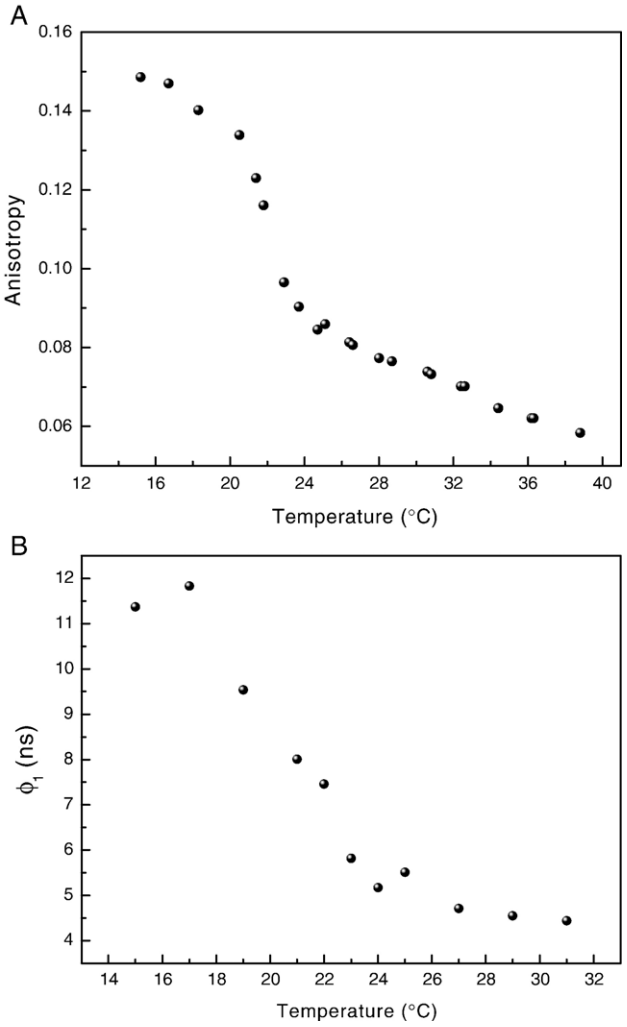

Fig. 9. Dependence with temperature of steady state anisotropy (A) and rotational correlation time (B) of AHBA (10 μM) in DMPC (0.5 mM) vesicles.

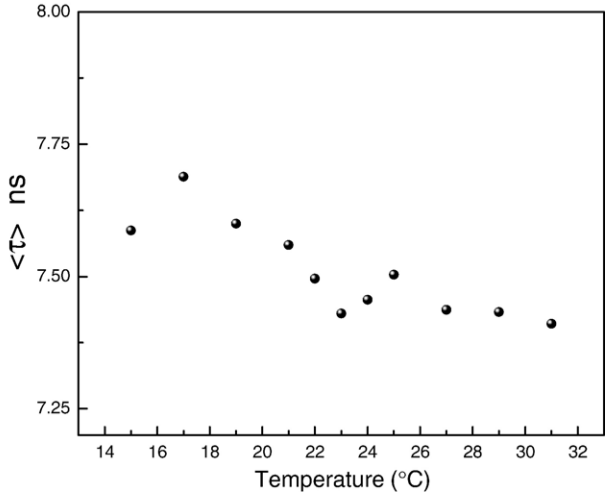

Fig. 8. Dependence with temperature of average lifetime of AHBA (10 μM) in DMPC (0.7 mM) vesicles.

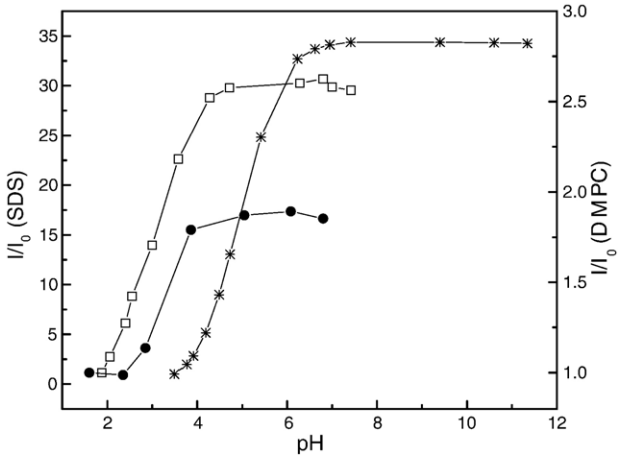

Fig. 10. Dependence with pH of fluorescence intensity of AHBA in SDS 40 mM (∗), DMPC 0.5 mM at 30 °C (□) and DMPC 0.5 mM at 16 °C (●). AHBA concentration 10 μM, in buffer, pH 7.4.

Table 4
pK values in the presence of micelles and vesicles and surface electric potential Ψ_S

	pK	ΔpK_{16}	ΔpK_{30}	$\Psi_{S\ 16}$ (mV)	$\Psi_{S\ 30}$ (mV)
DMPC 16 °C	3.26±0.05	–	–	–	–
DMPC 30 °C	2.98	–	–	–	–
SDS	4.95	1.69	1.97	−93.2	−108.7
CTAB	1.47	−1.79	−1.51	98.7	83.3
DPS	1.66	−1.60	−1.32	88.3	72.8

4.6. Interaction with DMPC vesicles: monitoring pH effects and surface potential

The amine group of the fluorophore *o*-Abz is titratable and the fluorescence properties of the molecule is dependent on the pH of the medium. At low pH's the amino group of the fluorophore protonates and the fluorescence intensity decreases. In buffer, the intensity and lifetime of AHBA aggregates did not modify in the pH range between 3.0 and 10.0. However, after dissolving in surfactant micelles, the fluorescence intensity of the probe was strongly dependent on the pH of the medium, as illustrated in Fig. 10 for the titration in the presence of SDS. From the curves of intensity versus pH we could determine the pK of the protonation of the fluorophore, which was dependent on the surfactant (Table 4). Similar observation was made for AHBA in the presence of DMPC vesicles (Table 4), both above and below the phase transition temperature.

As the probe is located in the micelles and vesicles, the pK's differ from the values obtained for the fluorophore free in solution. Differences in pK values reflect differences in local pH compared to the bulk pH, originating from the surface potential of micelles or vesicles [20]. As shown by Fornés et al., comparison of [21] the local pH_S with the bulk pH_b allows the calculation of surface potential ψ_S of micelles or vesicles, through

$$\psi_S = -2.3\frac{kT}{e}(pH_S - pH_b)$$

where k is the Boltzmann constant, equal to 1.281×10^{-23} J K^{-1}, T is the temperature and e is the electron charge, equal to $1.602\times10^{-}$super ^{19} C. In the calculations we used as pH_S the value of the pK for the probe inserted in the micelles and for pH_b, the bulk pH, the pK value obtained when the probe was inserted in the neutral DMPC vesicles. We suppose, thus, that the pK in the presence of neutral micelles is the same as would be obtained for the probe in the bulk. Such direct observation of the pK in the bulk was not possible due to the aggregation of AHBA in aqueous medium.

The values for the surface potential of SDS and CTAB micelles, shown in Table 4, are comparable to those obtained with the lipophilic probes derived from hydroxicoumarin [20]. It should be expected for the surface potential of DPS micelle values around zero. However we obtained a positive value for the potential surface. As the positive and negative charges of this zwitterionic surfactant are separated by three carbon atoms, it is possible that the aromatic ring of AHBA is positioned near to the charged nitrogen, in a region of positive potential.

5. Conclusions

Fluorescence and optical absorption results show that the newly synthesized compound dissolves in solvents like ethanol and cyclohexane and, due to the low solubility in water, forms aggregates in aqueous medium. In the presence of surfactants and phospholipids the spectral position of absorption and emission bands are typical of the probe in low polarity solvents. In the titration with surfactants the fluorescence intensity and lifetime increases, while steady state and rotational correlation times decreases, due to the disruption of aggregates formed in water and the insertion of the probe in the hydrophobic regions of the micelles of SDS, CTAB, HPS and DPS. The high association constant reveals the strong affinity of the probe with surfactants, independent of the state of charge of the micelles, in a process driven by the hydrophobic interactions between probe and surfactant. Several fluorescence parameters measured in the presence of DMPC vesicles demonstrate that the probe has also affinity to the lipid region of the bilayers, and is able to monitor phase transition between liquid crystalline and gel phases. The fluorescence of the probe is pH dependent and the pK for the titration of the benzoamino group is dependent on the charge of the head group of the surfactant micelles. Relating the differences in pK values with the differences in local pH, it has been shown that the AHBA probe is useful also to determine electric potential of micelles surface.

Acknowledgments

This work was supported by grants from the Fundação de Amparo à Pesquisa do Estado de São Paulo (FAPESP), Coordenação de Aperfeiçoamento de Pessoal do Ensino Superior (CAPES, Brasil) and Conselho Nacional de Desenvolvimento Científico e Tecnológico (CNPq, Brasil).

References

[1] A.S. Ito, R.F. Turchiello, I.Y. Hirata, M.H. Cezari, M. Meldal, L. Juliano, Fluorescent properties of amino acids labeled with *ortho*-aminobenzoic acid, Biospectroscopy 4 (1998) 395–402.
[2] J.R. Chagas, F.C. Portaro, I.Y. Hirata, P.C. Almeida, M.A. Juliano, L. Juliano, E.S. Prado, Determinants of the unusual cleavage specificity of lysyl-bradykinin-releasing kallikreins, Biochem. J. 306 (1995) 63–69.
[3] E. Del Nery, J.R. Chagas, M.A. Juliano, E.S. Prado, L. Juliano, Evaluation of the extent of the binding site in human tissue kallikrein by synthetic substrates with sequences of human kininogen fragments, Biochem. J. 312 (1995) 233–238.
[4] E.S. Souza, I.Y. Hirata, L. Juliano, A.S. Ito, End-to-end distribution distances in bradykinin observed by fluorescence energy transfer, Biochim. Biophys. Acta 1474 (2000) 251–261.
[5] D.C. Pimenta, I.L. Nantes, E.S. Souza, B. le Boniec, A.S. Ito, I.L.S. Tersariol, V. Oliveira, M.A. Juliano, L. Juliano, Interaction of heparin with internally quenched fluorogenic peptides derived from heparin-binding consensus sequences, kallistatin and anti-thrombin III, Biochem. J. 366 (2002) 435–446.
[6] A.S. Ito, E.S. Souza, S.R. Barbosa, C.R. Nakaie, Fluorescence study of conformational properties of melanotropins labeled with aminobenzoic acid, Biophys. J. 81 (2001) 1180–1189.
[7] R.F. Turchiello, M.T. Lamy-Freund, I.Y. Hirata, L. Juliano, A.S. Ito, *Ortho*-aminobenzoic acid as a fluorescent probe for the interaction between peptides and micelles, Biophys. Chemist. 73 (1998) 217–225.

[8] R.F. Turchiello, M.T. Lamy-Freund, I.Y. Hirata, L. Juliano, A.S. Ito, *Ortho*-aminobenzoic acid-labeled bradykinins in interaction with lipid vesicles: fluorescence study, Biopolymers 65 (2002) 336–346.
[9] I. Kalnina, I. Meirovics, A new fluorescent probe, ABM: properties and application in clinical diagnostics, J. Fluoresc. 9 (1999) 27–32.
[10] K. Nagy, S. Göktürk, L. Biczók, Effect of microenvironment on the fluorescence of 2-hydroxy-substituted Nile Red dye: a new fluorescent probe for the study of micelles, J. Phys. Chem., A 107 (2003) 8784–8790.
[11] M. Shannigrahi, S. Bagchi, Novel fluorescent probe as aggregation predictor and micro-polarity reporter for micelles and mixed micelles, Spectrochim. Acta, A 61 (2005) 2131–2138.
[12] Y. Singh, A. Gulyani, S. Bhattacharya, A new ratiometric fluorescence probe as strong sensor of surface charge of lipid vesicles and micelles, FEBS Lett. 541 (2003) 132–136.
[13] S.K. Ghosh, A. Pal, S. Kundu, M. Mandal, S. Nath, T. Pal, Emission behavior of 1-methylaminopyrene in aqueous solution of anionic surfactants, Langmuir 20 (2004) 5209–5213.
[14] M.J. Hope, M.B. Bally, G. Webb, P.R. Cullis, Production of large unilamellar vesicles by a rapid extrusion procedure. Characterization of size distribution, trapped volume and ability to maintain a membrane potential, Biochim. Biophys. Acta 812 (1985) 55–65.
[15] I.Z. Siemion, T. Wieland, The amide-aromatic-ring system. An inherently dissymetric chromophore, Tetrahedron 33 (1977) 155–157.
[16] M. Takara, A.S. Ito, General and specific solvent effects in optical spectra of *ortho*-aminobenzoic acid, J. Fluoresc. 15 (2005) 171–177.
[17] W.H. Melhuish, Quantum efficiencies of fluorescence of organic substances: effect of solvent and concentration of the fluorescent solute, J. Phys. Chem. 65 (2) (1961) 229–235.
[18] R. Ray, Fluorescence quenching of *o*-aminobenzoic acid by ethylene trithiocarbonate in aqueous micellar media, J. Photochem. Photobiol., A 76 (1993) 115–120.
[19] J. Katsaras, T. Gutberlet, Lipid Bilayers: Structure and Interactions, Springer Verlag, Berlin, 2001.
[20] M. Fernandez, P. Fromherz, Lipoid pH indicators as probes of electrical potential and polarity in micelles, J. Phys. Chem. 81 (1977) 1755–1761.
[21] J.A. Fornés, A.S. Ito, R. Curi, J. Procopio, pH fluctuations in unilamellar vesicles, Phys. Chem. Chem. Phys. 1 (1999) 5133–5138.